Stress-dependent cardiac remodeling occurs in the absence of microRNA-21 in mice

David M. Patrick,[1] Rusty L. Montgomery,[2] Xiaoxia Qi,[1] Susanna Obad,[3] Sakari Kauppinen,[3,4] Joseph A. Hill,[5] Eva van Rooij,[2] and Eric N. Olson[1]

[1]Department of Molecular Biology, University of Texas Southwestern Medical Center, Dallas, Texas, USA. [2]miRagen Therapeutics, Boulder, Colorado, USA. [3]Santaris Pharma, Hørsholm, Denmark. [4]Copenhagen Institute of Technology, Aalborg University, Ballerup, Denmark. [5]Department of Internal Medicine, University of Texas Southwestern Medical Center, Dallas, Texas, USA.

MicroRNAs inhibit mRNA translation or promote mRNA degradation by binding complementary sequences in 3′ untranslated regions of target mRNAs. MicroRNA-21 (miR-21) is upregulated in response to cardiac stress, and its inhibition by a cholesterol-modified antagomir has been reported to prevent cardiac hypertrophy and fibrosis in rodents in response to pressure overload. In contrast, we have shown here that miR-21–null mice are normal and, in response to a variety of cardiac stresses, display cardiac hypertrophy, fibrosis, upregulation of stress-responsive cardiac genes, and loss of cardiac contractility comparable to wild-type littermates. Similarly, inhibition of miR-21 through intravenous delivery of a locked nucleic acid–modified (LNA-modified) antimiR oligonucleotide also failed to block the remodeling response of the heart to stress. We therefore conclude that miR-21 is not essential for pathological cardiac remodeling.

Introduction

The heart responds to injury and hemodynamic overload by promoting myocyte hypertrophy, reexpressing a fetal gene program, and remodeling of the extracellular matrix (1). MicroRNAs (miRNAs), which cause translational inhibition or degradation of specific mRNAs, play critical roles in tissue responses to stress and are mis-expressed in diseased murine and human hearts (2–8). Gain and loss of function in mice have implicated miRNAs in diverse aspects of cardiac function and dysfunction (refs. 3, 7, 9; reviewed in ref. 10).

miR-21 has been implicated in a variety of disorders and is highly upregulated during cardiac remodeling (refs. 7–9, 12; reviewed in refs. 5, 11), but the precise functions of miR-21 in cardiac stress responses have been unclear. In cultured myocytes, miR-21 has been reported to be both pro- and anti-hypertrophic (13, 14). Thum et al. reported that knockdown of miR-21 through systemic delivery of cholesterol-modified antisense oligonucleotides (antagomirs) prevented cardiac hypertrophy and fibrosis in response to pressure overload induced by transaortic constriction (TAC). These salutary effects were attributed to the derepression of the miR-21 target transcript Sprouty-1 (*Spry1*), which inhibits MAP kinase signaling specifically in cardiac fibroblasts (9).

We show here that genetic deletion of miR-21 or acute inhibition of miR-21 through systemic delivery of a locked nucleic acid–modified (LNA-modified) antimiR oligonucleotide does not alter the pathological responses of the heart to pressure overload or other stresses. We conclude that miR-21 is not required for cardiac hypertrophy, fibrosis, or loss of contractile function in response to acute or chronic injury in mice.

Results and Discussion

Generation of Mir21⁻/⁻ mice. To generate *Mir21⁻/⁻* mice, we introduced loxP sites at both ends of pre-miR-21 through homologous

recombination (Supplemental Figure 1A; supplemental material available online with this article; doi:10.1172/JCI43604DS1). Global deletion of miR-21 was achieved by breeding *Mir21ᶠˡ/⁺* mice to mice expressing CAG-Cre. Mice homozygous for miR-21 deletion were obtained at predicted Mendelian ratios (Table 1). Deletion of miR-21 was confirmed by PCR, Southern blot, and Northern blot analyses (Supplemental Figure 1, B–D). Regulatory sequences for the *Mir21* gene are located adjacent to the penultimate intron of the *Tmem49* gene (Supplemental Figure 1A) (15). *Tmem49* mRNA expression was unaltered in *Mir21⁻/⁻* animals (Supplemental Figure 1, A and E, and Supplemental Figure 2). Homozygous mutant mice displayed no overt abnormalities. Similarly, mutant mice displayed no abnormalities in heart size, structure, or cardiac contractility and no modification of protein levels of predicted miR-21 target transcripts encoding Pdcd4 and Spry1 (Supplemental Figure 1, F and G).

Cardiac stress responses are unperturbed in Mir21-null mice. To investigate the potential involvement of miR-21 in pathological cardiac remodeling, we subjected *Mir21⁻/⁻* mice to 4 different cardiac stresses: (a) acute pressure overload due to TAC (16); (b) chronic calcineurin activation (17); (c) infusion of Ang II, which induces cardiac remodeling through myocyte-autonomous mechanisms and secondary hypertension (18); and (d) myocardial infarction (MI) due to ligation of the proximal left anterior descending (LAD) coronary artery.

WT and *Mir21⁻/⁻* mice showed comparable pathological remodeling in response to all 4 stresses (Figure 1, A and B). Northern blot analysis for miR-21 revealed upregulation in WT myocardium in response to all stresses and confirmed the absence of miR-21 expression in mutant mice (Figure 1C). WT and *Mir21⁻/⁻* animals showed a comparable fibrotic response and upregulation of collagen and fetal cardiac genes (Figure 1D and Figure 2A). Functional analysis by echocardiography after TAC also indicated no differences between the two genotypes (Supplemental Figure 3). *Mir21⁻/⁻* animals displayed a mildly exaggerated increase in heart weight/body weight (HW/BW) ratio in response to Ang II when compared with Ang II–treated WT animals, suggesting a modest susceptibility to Gq-induced cardiac hypertrophy. MI induced by

Table 1
Mir21⁻/⁻ mice are born at predicted Mendelian ratios

miR-21 genotype (93 animals)	Expected, no. (%)	Observed, no. (%)
WT	23 (25%)	19 (20%)
Heterozygous	47 (50%)	55 (60%)
KO	23 (25%)	19 (20%)

LAD occlusion resulted in pronounced scar formation at the apex and free wall of the left ventricular chamber. The extent of scar formation and remodeling was indistinguishable between mice of the two genotypes (Figure 1A and Supplemental Figure 4A). Quan-

tification of infarct size revealed no significant differences between WT and *Mir21⁻/⁻* mice (Supplemental Figure 4B).

miR-21 was reported to influence cardiac remodeling by regulating MAP kinase signaling and phosphorylation of Erk (9). However, Western blot analysis showed a stress-dependent increase in phospho-Erk even in the absence of miR-21 (Figure 2B). Thus, the chronic deletion of miR-21 does not alter myocardial MAP kinase signaling in response to cardiac stress.

Based on prior studies (7–9, 19, 20), we anticipated that miR-21 would be involved in cardiac hypertrophy and fibrosis. The failure of genetic deletion of miR-21 to diminish these cardiac stress responses might be explained by compensatory mechanisms activated in the persistent absence of miR-21. To further explore the potential involvement of miR-21 in the responses of the heart to stress, we inhibited miR-21 acutely using an antimiR approach.
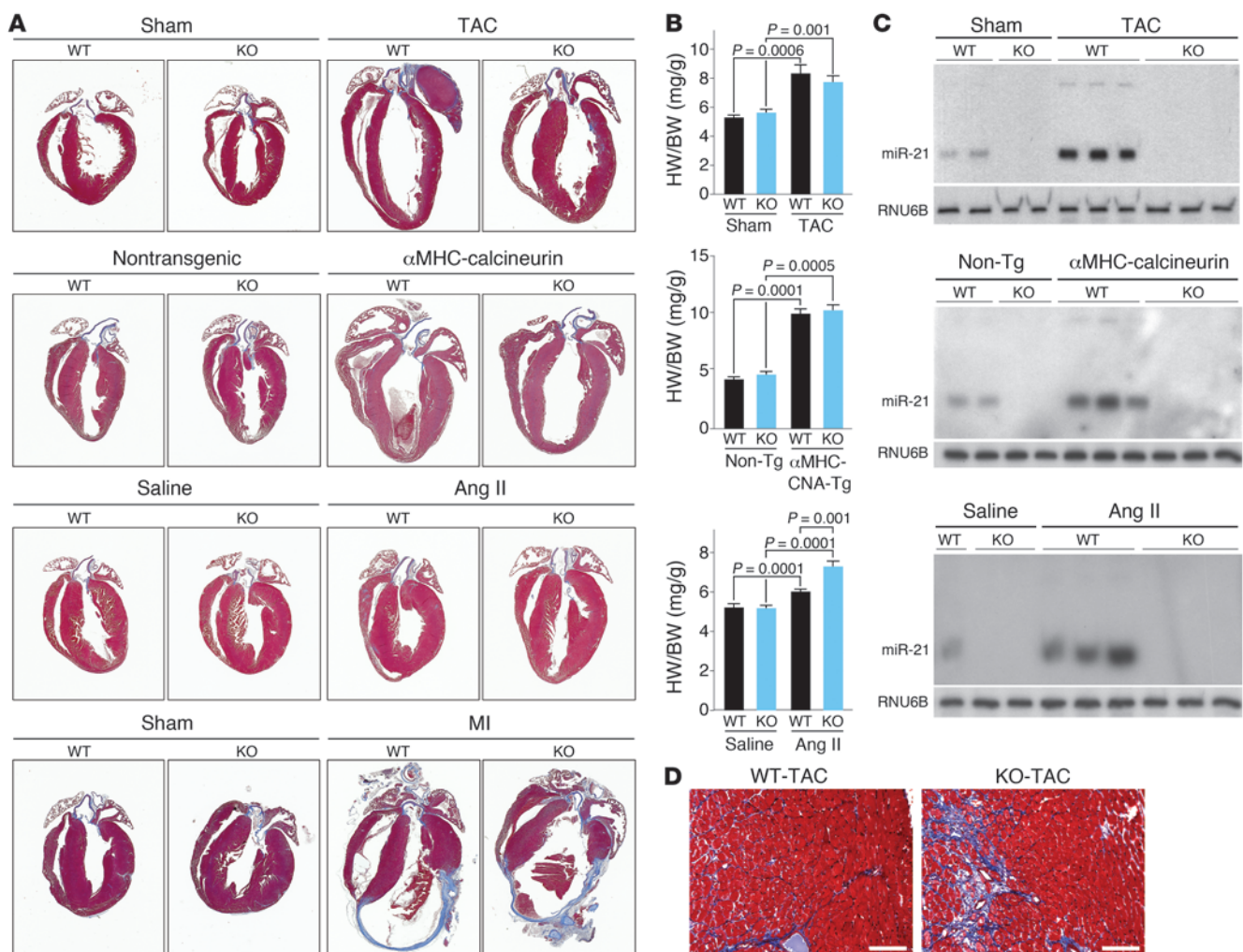

Figure 1
miR-21 is not required for cardiac hypertrophy or fibrosis in response to stress. (**A**) Trichrome staining on cardiac sections of WT and *Mir21⁻/⁻* (KO) animals after TAC, transgenic expression of calcineurin, chronic Ang II infusion, or MI, as indicated. Histological analysis shows that miR-21 deletion has no effect on cardiac remodeling in response to stress, based on cardiac hypertrophy and fibrosis. (**B**) HW/BW ratios of mice of the indicated genotypes in response to the indicated stresses. HW/BW data shown for TAC experiments represent *n* = 9 for WT sham, *n* = 10 for KO sham, *n* = 14 for WT TAC, and *n* = 13 for KO TAC. HW/BW data shown for calcineurin overexpression represent *n* = 4 WT non-Tg, *n* = 3 KO non-Tg, *n* = 4 WT Tg, and *n* = 3 KO Tg. HW/BW data shown for Ang II infusion represent *n* = 9 WT saline, *n* = 8 KO saline, *n* = 11 WT Ang II, and *n* = 7 KO Ang II. (**C**) Detection of miR-21 expression in hearts of mice of the indicated genotypes in response to the indicated stresses by Northern blot analysis. RNU6B was detected as loading control. CNA, calcineurin. (**D**) Trichrome staining of hearts of the indicated genotypes 3 weeks following TAC surgery. Scale bars: 100 μm.
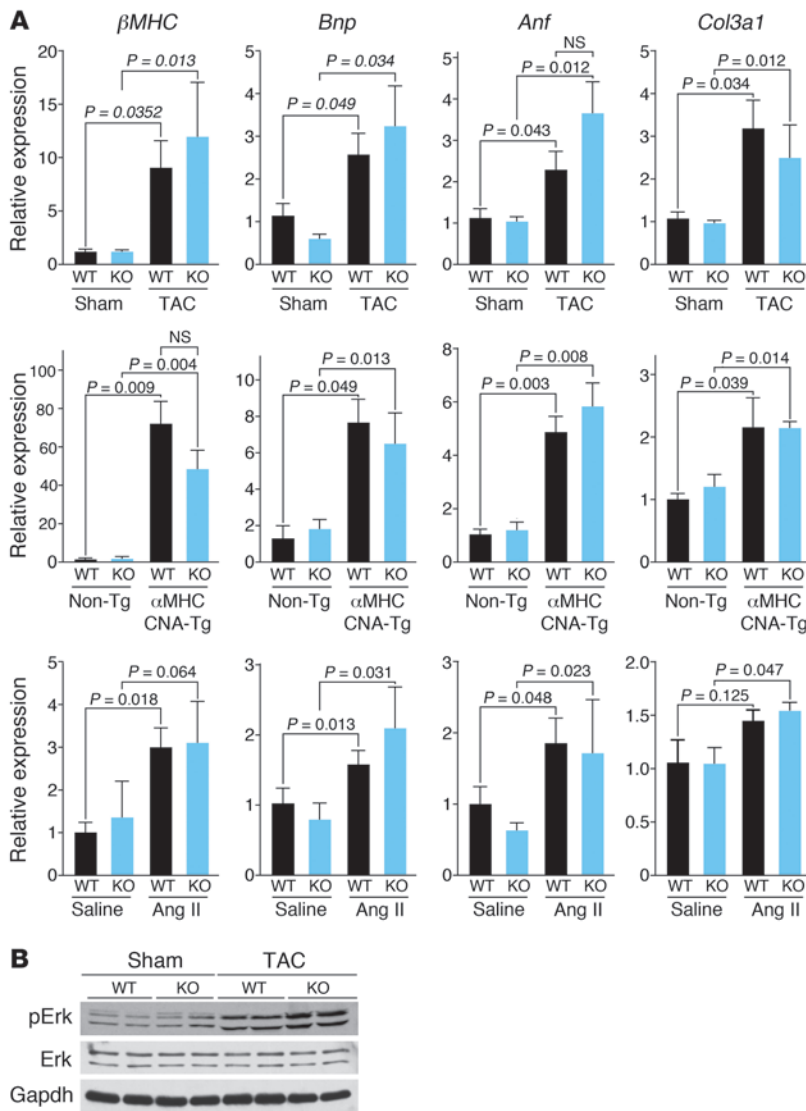
Figure 2
miR-21 deletion does not alter the expression of cardiac stress markers. (**A**) Quantitative real-time PCR analysis for hearts of the indicated genotypes in response to the indicated stresses shows no effect on cardiac gene expression during stress in the absence of miR-21. Gene expression data shown for TAC experiments represent $n = 6$ for WT sham, $n = 6$ for KO sham, $n = 10$ for WT TAC, and $n = 10$ for KO TAC. Data shown for calcineurin overexpression represent $n = 3$ WT non-Tg, $n = 3$ KO non-Tg, $n = 3$ WT Tg, and $n = 3$ KO Tg. Data shown for Ang II infusion represent $n = 3$ WT saline, $n = 3$ KO saline, $n = 4$ WT Ang II, and $n = 3$ KO Ang II. (**B**) Western blot analysis indicates a comparable stress-induced increase in phospho-ERK for both WT and $Mir21^{-/-}$ (KO) hearts in response to TAC.

LNA control had no effect (Supplemental Figure 5C). Inhibition of miR-21 with antimiR-21 caused an increase in the miR-21 target Pdcd4, while a comparable dose of the LNA scramble control had no effect (Supplemental Figure 5D).

Based on these data, we used antimiR-21 to determine whether inhibition of miR-21 during cardiac stress would influence cardiac remodeling. Animals were dosed with 25 mg/kg of antimiR-21 or LNA scramble control as described in Methods. Histological examination and measurements of HW/BW ratio indicated that cardiac hypertrophy was comparable in untreated animals and animals treated with antimiR-21 (Figure 3, A and B, and Supplemental Figure 6B). TAC caused a 2.7-fold increase in miR-21 expression 21 days after surgery compared with sham-operated animals. AntimiR-21 effectively antagonized miR-21, whereas treatment with LNA control had no effect on cardiac miR-21 levels (Figure 3, C and D). Notably, Northern blot analysis using an LNA probe complementary to the entire miR-21 sequence revealed a shifted band only in samples harvested from antimiR-21–treated mice. These data suggest that mature miR-21 is sequestered in a slower-migrating heteroduplex with the antimiR-21 bound to the seed sequence.

Echocardiography showed no difference in cardiac function between groups, and there was no difference in β–myosin heavy chain (βMHC) upregulation (Figure 3E and Supplemental Figure 7). Western blot analysis showed miR-21 inhibition to have no effect on Erk phosphorylation in response to stress (Figure 3F). However, Western blot analysis showed derepression of the miR-21 target Pdcd4 after antimiR-21 treatment, indicating antagonism of miR-21 in the heart (Figure 3G).

Similarly, intravenous delivery of antimiR-21 for 3 days prior to chronic Ang II administration inhibited the upregulation of miR-21) but did not alter the extent of cardiac hypertrophy or remodeling compared with LNA control or saline-treated animals (Figure 3, H–J, and Supplemental Figure 6C). Expression analysis of βMHC, Col3a1, and Col1a2 also showed no difference between groups (Supplemental Figure 7).

We conclude that LNA-antimiR oligonucleotides can functionally inhibit cardiac miRNAs upon systemic delivery into

LNA-mediated knockdown of miR-21. Therapeutic efficacy of LNA-antimiR technology has recently been reported (21, 22). As a consequence of the high binding affinity of LNA-containing antisense oligonucleotides, biological activity is attained with shorter LNA oligonucleotides (S. Obad et al., unpublished observations). To test whether miR-21 could be inhibited with LNA-modified antimiRs, we used an 8-nt fully LNA-modified phosphorothioate oligonucleotide complementary to the seed region of miR-21 (Supplemental Figure 5A). The activity of a luciferase reporter fused to the 3′ UTR of the miR-21 target transcript *Pdcd4* (19) was repressed by increasing concentrations of miR-21 in Cos cells, whereas cotransfection of this reporter with antimiR-21 derepressed the *Pdcd4*-luciferase reporter, which we attribute to functional inhibition of endogenous miR-21 (Supplemental Figure 5B).

To examine the ability of antimiR-21 to repress miR-21 levels in vivo, we exposed animals to TAC to induce miR-21 and 6 weeks later injected them intravenously with antimiR-21 or a scrambled control (Supplemental Figure 6A). While TAC induced cardiac miR-21 expression, systemic administration of antimiR-21 resulted in dose-dependent inhibition of miR-21 expression in the heart, whereas the
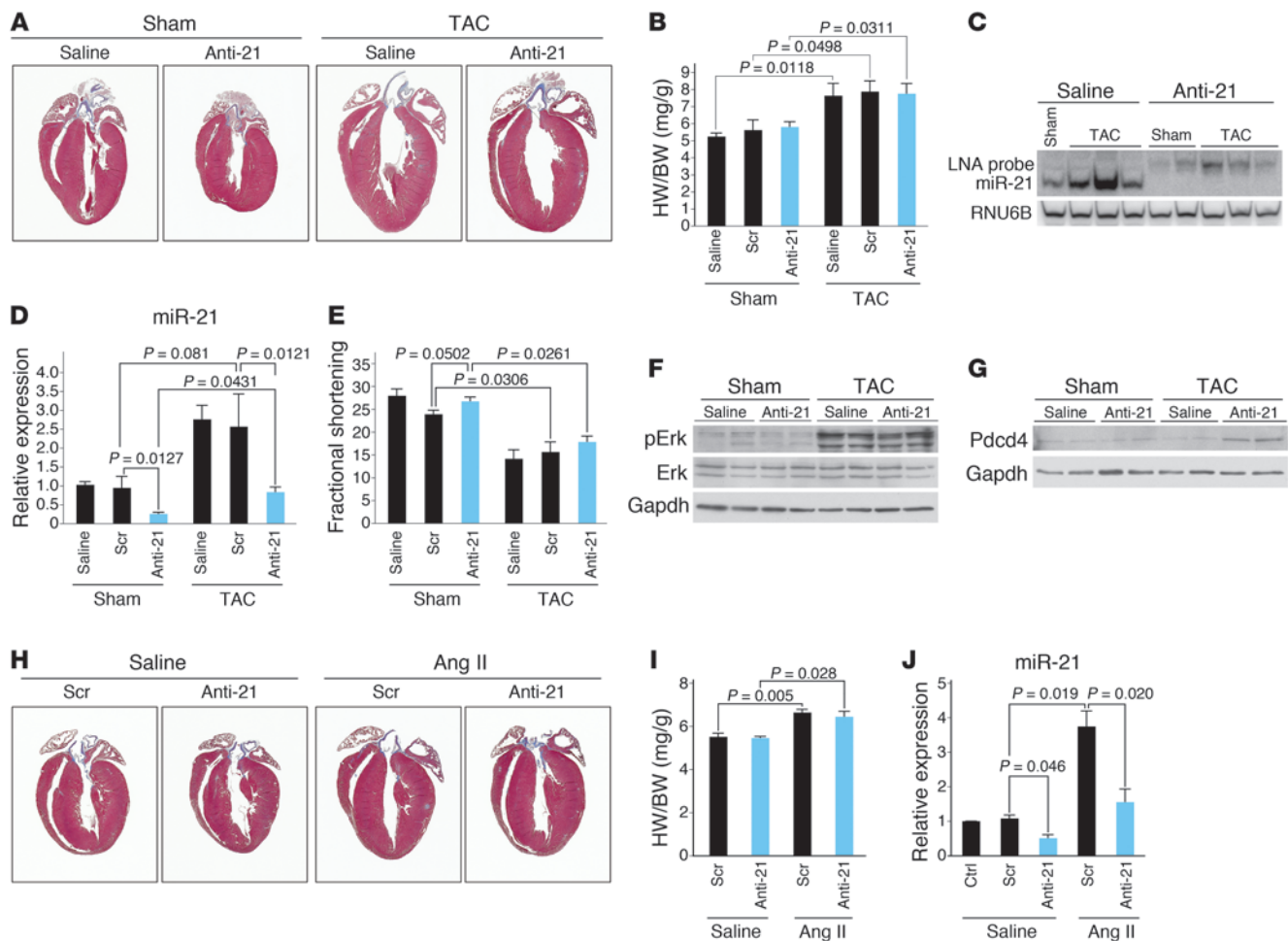
Figure 3
Cardiac stress response after antimiR-21 treatment. (**A**) Trichrome-stained sections of hearts show that animals treated with both saline and antimiR-21 (Anti-21) display induction of cardiac hypertrophy upon TAC. (**B**) HW/BW ratios of mice treated as indicated. HW/BW data represent $n = 6$ for sham conditions and $n = 12$ for TAC conditions. (**C**) Northern blot analysis for miR-21 in cardiac tissue of animals treated as indicated. The upshift reflects a heteroduplex between miR-21 and antimiR-21. RNU6B was a loading control. (**D**) Real-time RT-PCR analysis of miR-21 expression in cardiac tissue after the indicated treatments. Data represent $n = 5$ for sham conditions and $n = 10$ for TAC conditions. Scr, scrambled control. (**E**) Functional analysis of the heart represented by fractional shortening. Data represent $n = 6$ for sham conditions and $n = 12$ for TAC conditions. (**F**) Western blot analysis indicates a stress-induced increase in phospho-Erk for saline- and antimiR-21–treated mice in response to TAC. (**G**) Western blot analysis shows an increase in Pdcd4 in antimiR-21–treated mice in response to TAC. (**H**) Trichrome-stained sections of hearts from animals treated as indicated. Animals treated with both LNA scrambled control and antimiR-21 display induction of cardiac hypertrophy upon Ang II infusion. (**I**) HW/BW ratios of mice treated as indicated. Ratios represent $n = 3$ for Scr Saline, $n = 4$ for Anti-21 saline, $n = 3$ for Ang II saline, and $n = 5$ for Anti-21 Ang II. (**J**) Real-time RT-PCR analysis of miR-21 expression in cardiac tissue of animals after the indicated treatments using untreated C57BL/6 cardiac tissue as control (Ctrl).

mice, but inhibition of miR-21 by this approach does not prevent pathological cardiac remodeling in response to pressure overload or Ang II administration. Our results differ from those of Thum et al., who concluded, based on antagomir-21–knockdown studies in mice, that miR-21 was essential for cardiac hypertrophy and fibrosis in response to pressure overload (9). How might these differences be reconciled? The failure of genetic deletion of miR-21 to diminish cardiac hypertrophy or fibrosis in response to stress might be explained by compensatory mechanisms activated in the persistent absence of miR-21. In this regard, and given the chronic nature of heart failure in humans, therapeutic strategies designed to treat this condition should display long-term efficacy.

It is conceivable that variations in the level of cardiac stress imposed by TAC in the two studies could account for differential responsiveness to miR-21 inhibition, although the two studies showed comparable reduction in cardiac contractility and increased phospho-Erk in response to the procedure. Regarding the disparity between the effects of cholesterol-conjugated antagomirs and unconjugated LNA-modified antimiR-21 on cardiac remodeling, it is worth noting that we injected LNA-antimiRs via the tail vein, whereas Thum et al. injected antagomir via the jugular vein (9). There is also a possibility that cholesterol-conjugated chemistry has a cardioprotective effect, or antagomirs might also be more effective than LNA-modified antimiRs at inhibiting miR-21 function in cardiac fibroblasts in vivo. Irrespective of pos-

sible experimental variations between our study and that of Thum et al., our finding that pathological cardiac remodeling in response to four different stresses in vivo is unaffected by genetic deletion of miR-21 seems to rule out an absolute requirement for this miRNA as a driver of heart disease.

Although we were unable to identify an important role for miR-21 in pathological cardiac remodeling, miR-21–knockout mice display a reduced susceptibility to lung tumorigenesis in response to K-ras activation, which reflects the upregulation of multiple antagonists of the Ras/MAP kinase signaling pathway in these mice (23). Thus, miR-21 clearly possesses modulatory activity for pathogenic signaling pathways in vivo, and such mechanisms can be perturbed upon genetic deletion of miR-21 (23).

Methods

Experimental procedures are described in detail in Supplemental Methods.

Generation of miR-21 mutant mice. See Supplemental Methods.

Northern blotting. Analyses were performed as previously described (3). See Supplemental Methods for details.

Mouse models of cardiac remodeling. Mice underwent sham or TAC surgery as previously described (16). Mice were bred to animals harboring the αMHC-calcineurin transgene as previously described (17). To mimic MI, animals were subjected to LAD occlusion or sham surgery. Ang II infusions were performed at 2 mg/kg/d for 14 days. See Supplemental Methods for details.

LNA-based knockdown of miR-21. The LNA-antimiR or LNA scrambled control oligonucleotides were injected at the indicated time points and indicated doses. See Supplemental Methods for details of LNA synthesis and treatment.

RT-PCR, real-time RT-PCR analysis, and Western blotting. Gene expression was quantitated using Taqman probes purchased from Applied Biosystems. Primers to analyze *Tmem49* expression are provided in Supplemental Methods. Western blotting was performed as described in Supplemental Methods.

Thoracic echocardiography. Analyses were performed using a Visual Sonics Vevo 770 Ultrasound (Visual Sonics) and a 30-MHz linear array transducer. See Supplemental Methods for details.

Animal care. All animal procedures were approved by the Institutional Animal Care and Use Committee at UT Southwestern.

Statistics. We evaluated statistical significance by 2-tailed Student's *t* test, with $P < 0.05$ regarded as significant. We show all data as mean ± SEM.

Address correspondence to: Eric N. Olson, Department of Molecular Biology, UT Southwestern Medical Center at Dallas, 5323 Harry Hines Blvd., Dallas, Texas 75390-9148, USA. Phone: 214.648.1187; Fax: 214.648.1196; E-mail: eric.olson@utsouthwestern.edu. Or to: Eva van Rooij, miRagen Therapeutics, Inc., 6200 Lookout Rd., Boulder, Colorado 80301, USA. Phone: 303.531.5952; Fax: 303.531.5094; E-mail: evanrooij@miragenrx.com.

1. Hill JA, Olson EN. Cardiac plasticity. *N Engl J Med*. 2008;358(13):1370–1380.
2. Williams AH, et al. MicroRNA-206 delays ALS progression and promotes regeneration of neuromuscular synapses in mice. *Science*. 2009; 326(5959):1549–1554.
3. van Rooij E, Sutherland LB, Qi X, Richardson JA, Hill J, Olson EN. Control of stress-dependent cardiac growth and gene expression by a microRNA. *Science*. 2007;316(5824):575–579.
4. Xin M, et al. MicroRNAs miR-143 and miR-145 modulate cytoskeletal dynamics and responsiveness of smooth muscle cells to injury. *Genes Dev*. 2009; 23(18):2166–2178.
5. Selcuklu SD, Donoghue MT, Spillane C. miR-21 as a key regulator of oncogenic processes. *Biochem Soc Trans*. 2009;37(pt 4):918–925.
6. Thum T, et al. MicroRNAs in the human heart: a clue to fetal gene reprogramming in heart failure. *Circulation*. 2007;116(3):258–267.
7. van Rooij E, et al. A signature pattern of stress-responsive microRNAs that can evoke cardiac hypertrophy and heart failure. *Proc Natl Acad Sci U S A*. 2006;103(48):18255–18260.
8. van Rooij E, et al. Dysregulation of microRNAs after myocardial infarction reveals a role of miR-29 in cardiac fibrosis. *Proc Natl Acad Sci U S A*. 2008; 105(35):13027–13032.
9. Thum T, et al. MicroRNA-21 contributes to myocardial disease by stimulating MAP kinase signalling in fibroblasts. *Nature*. 2008;456(7224):980–984.
10. Small EM, Frost RJ, Olson EN. MicroRNAs add a new dimension to cardiovascular disease. *Circulation*. 2010;121(8):1022–1032.
11. Krichevsky AM, Gabriely G. miR-21: a small multi-faceted RNA. *J Cell Mol Med*. 2009;13(1):39–53.
12. Cheng Y, Zhang C. MicroRNA-21 in cardiovascular disease. *J Cardiovasc Transl Res*. 2010;3(3):251–255.
13. Cheng Y, et al. MicroRNAs are aberrantly expressed in hypertrophic heart: do they play a role in cardiac hypertrophy? *Am J Pathol*. 2007;170(6):1831–1840.
14. Tatsuguchi M, et al. Expression of microRNAs is dynamically regulated during cardiomyocyte hypertrophy. *J Mol Cell Cardiol*. 2007;42(6):1137–1141.
15. Fujita S, et al. miR-21 Gene expression triggered by AP-1 is sustained through a double-negative feedback mechanism. *J Mol Biol*. 2008;378(3):492–504.
16. Hill JA, et al. Cardiac hypertrophy is not a required compensatory response to short-term pressure overload. *Circulation*. 2000;101(24):2863–2869.
17. Molkentin JD, et al. A calcineurin-dependent transcriptional pathway for cardiac hypertrophy. *Cell*. 1998;93(2):215–228.
18. Schluter KD, Wenzel S. Angiotensin II: a hormone involved in and contributing to pro-hypertrophic cardiac networks and target of anti-hypertrophic cross-talks. *Pharmacol Ther*. 2008; 119(3):311–325.
19. Cheng Y, et al. Ischaemic preconditioning-regulated miR-21 protects heart against ischaemia/reperfusion injury via anti-apoptosis through its target PDCD4. *Cardiovasc Res*. 2010;87(3):431–439.
20. Dong S, et al. MicroRNA expression signature and the role of microRNA-21 in the early phase of acute myocardial infarction. *J Biol Chem*. 2009; 284(43):29514–29525.
21. Elmen J, et al. LNA-mediated microRNA silencing in non-human primates. *Nature*. 2008; 452(7189):896–899.
22. Lanford RE, et al. Therapeutic silencing of microRNA-122 in primates with chronic hepatitis C virus infection. *Science*. 2010;327(5962):198–201.
23. Hatley ME, et al. Modulation of K-ras-dependent lung tumorigenesis by MicroRNA-21. *Cancer Cell*. 2010;18(3):282–293.